Theor Chem Acc (2004) 111:264–269
DOI 10.1007/s00214-003-0516-5

Theoretical
Chemistry Accounts

Regular article

Surface-enhanced Raman spectra of pyridine and pyrazolide on silver colloids: chemical and electromagnetic effects

Maurizio Muniz-Miranda[1,2], **Gianni Cardini**[1,2], **Vincenzo Schettino**[1,2]

[1] Dipartimento di Chimica, Università di Firenze, 50019, Florence, Italy
[2] European Laboratory for Non-linear Spectroscopy (LENS), Polo Scientifico, Sesto Fiorentino, 50019, Florence, Italy

Received: 10 March 2003 / Accepted: 30 April 2003 / Published online: 5 December 2003

Abstract. The surface-enhanced Raman spectra of pyridine and pyrazolide adsorbed on silver colloids are discussed with the help of a density functional theory calculation, based on a mixed functional. The ligand–surface interaction is modelled as an adduct of pyridine and pyrazolide with a single Ag atom or with a small Ag cluster. It is found that the model adduct satisfactorily reproduces the relative Raman intensities of adsorbed pyridine, while the same is not the case for pyrazolide. From the analysis of the excitation profiles the observed behaviour is correlated with the relative importance of the chemical and electromagnetic effects.

Keywords: DFT – SERS – Colloid – Silver

Introduction

The enhancement mechanism of the Raman scattering cross-section in the surface-enhanced Raman scattering (SERS) experiment has been discussed extensively [1, 2, 3]. It is generally understood that there are two main contributions to the surface Raman enhancement. The so-called electromagnetic effect involves the enhancement of the electric field at the interface and the resonance with the surface plasmon absorption (SPA) band due to the excitation of the conduction electrons localised at the metal surface, producing an enhancement of the Raman signal by as much as 6 orders of magnitude. The electromagnetic effect causes in most cases a uniform enhancement of the Raman intensities and the actual appearance of the spectrum is related to surface-selection rules [4], depending on the orientation of the scattering molecules relative to the surface. The so-called chemical effect arises when the ligand is chemically adsorbed on the metal forming chemical bonds with the active sites (adatoms) of the surface and the exciting line is in resonance with the charge-transfer band of the ligand–surface adduct. Although the enhancement factor due to the chemical effect is much smaller (at most 10^2) [5, 6], its influence on the observed spectra can be substantial. As a matter of fact, the SERS spectra of adsorbed species should be discussed by comparison with a reference system, which in the case of chemisorption is the ligand–surface complex, whose vibrational frequencies can differ appreciably from those of the free ligand. In recent papers [7, 8, 9] it has been shown that the ligand–surface adducts can, as a first approximation, be modelled as a complex of the molecule with one metal atom or with a small cluster of metal atoms. The model successfully reproduced the frequency shifts of phthalimide [7], 2-mercaptobenzoxazole [8] and pyrazolide (Pz^-) [9] adsorbed on silver. The purpose of the present paper is to apply the same type of modelling of the ligand–surface chemical interaction to investigate if the relative intensities are also affected significantly. The approach is applied to the SERS spectra of pyridine (Py) and Pz^- adsorbed on silver colloids. It is shown that the behaviour of the two systems is distinctly different: with the help of the SERS excitation profiles these differences can be interpreted as arising from different contributions of the electromagnetic and chemical effects.

Experimental

Preparation of the samples

Stable Ag hydrosols were prepared according to Creighton's procedure [10] and aged 1 week to prevent the formation of reduction products [11]. Then, Py (Aldrich, purity 99.9 + %), or pyrazole (Aldrich, purity above 99%) purified twice by vacuum sublimation, was added (10^{-3} M concentration) to the silver colloids. A small amount of NaCl (5×10^{-4} M) was added to the Ag/Py hydrosol to observe the weak SERS bands of the ligand. $Ag(I)Py_2NO_3$ was prepared by dissolving $AgNO_3$ in hot Py in a 1:2 molar ratio,

---

Contribution to the Jacopo Tomasi Honorary Issue

Correspondence to: Vincenzo Schettino
e-mail: vincenzo.schettino@unifi.it

according to Cooney's procedure [12]. An Ag(I)/Pz$^-$ complex was obtained by mixing pyrazole with $AgNO_3$ in aqueous solution with NH_3, according to Buchner's method [13].

UV–vis absorption measurements

The UV–vis absorption spectra were measured with a Cary 5 spectrophotometer. The absorption spectra of the Ag colloids show an intense band at about 390 nm, due to the plasmon resonance of small metal particles (around 15 nm, as average diameter). In the presence of the ligand the silver colloidal particles undergo aggregation, resulting in the occurrence of a secondary plasmon band at longer wavelength. The degree of aggregation of the silver colloids was monitored by the relative intensities of the two plasmon absorption bands.

Raman measurements

Raman measurements were performed using a Jobin-Yvon HG-2S monochromator, a cooled RCA-C31034A photomultiplier and a data acquisition facility. SERS data were obtained with exciting lines supplied by Ar^+ and Kr^+ lasers, corrected to account for monochromator and photomultiplier efficiency and normalised to the Raman scattering of a KNO_3 water solution as external standard. The Raman spectra of the Ag(I) coordination compounds, as solid samples, were measured using a defocused laser beam and a rotating device to avoid thermal effects.

Calculation method

All the ab initio calculations were performed with the Gaussian98 package [14], using the combination of the B3LYP hybrid exchange correlation functional [15, 16] along with the Lanl2DZ basis set. This basis consists of the Dunning/Huzinaga full double zeta [17] on first-row atoms and of the Los Alamos pseudopotential for core electrons plus a double-zeta basis for valence electrons [18]. The structures were optimised with a tight criterion and the harmonic frequencies were calculated using an improved grid in the calculation of the integrals [Integral(Grid = 199974)]. A uniform scaling factor of 0.9833 was adopted for all the computed frequencies of the vibrational modes, as done recently by Aroca et al. [7] for phthalimide adsorbed on silver.

The Raman intensities of the Q_k vibrational modes, computed on the basis of the double harmonic approximation, i.e. without taking into account the electric and mechanical anharmonicities, correspond to spatially-averaged values according to the usual formula reported in standard textbooks [19]. The derivatives of the molecular polarisability with respect to the atomic displacements are considered as a response to an applied external electric field of 0.00189 au; hence, the intensities depend only on the variation of the molecular polarisability due to the molecular vibration or rotation. This calculation approach should allow Raman intensities to be reproduced with good accuracy in conditions far from the resonance of the exciting light with the electronic transitions. On the other hand, all the Raman spectra were measured using visible laser lines, whereas Py, Pz$^-$ and their corresponding Ag(I) coordination compounds absorb in the UV region.

Results and discussion

As discussed in the following, calculations of the Raman frequencies and intensities were carried on the silver complexes of Py and Pz$^-$, called Py/Ag$^+$ and Pz$^-$(Ag$_3$)$^+$, respectively. The optimised structure of Pz$^-$(Ag$_3$)$^+$ is shown in Fig. 1, where it can be seen that the cluster is arranged in a triangular structure with Ag–Ag distances close to the distances observed in bulk silver. The effective atomic charges were evaluated by natural bond orbital analysis and are reported in Table 1. For the complexes of both Py and Pz$^-$ the interaction with the metal surface results in a negative charge transfer towards the nitrogen and silver atoms, in order to form molecule–Ag bonds. In the case of Pz$^-$ the negative charge transferred to the metal cluster is concentrated exclusively on the silver atom that is more distant from the ligand. The Py–Ag bond turns out to be stronger than those involving Pz$^-$, as evidenced from the calculated bond lengths (2.176 Å for Py, 2.232 Å for Pz$^-$).

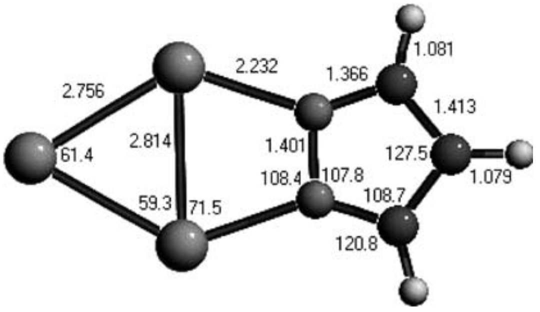

Fig. 1. Optimised structure of pyrazolide/(Ag$_3$)$^+$ complex. Bond distances in angstroms; bond angles in degrees

Pyridine

It is well known [10, 20, 21] that the SERS spectra may reach the highest intensities when the exciting wavelength falls within the envelope of the SPA band, owing to the excitation of the conduction electrons localised at the metal surface. The electromagnetic effect strongly depends on the degree of roughness of the surface, whereas it is independent of the properties of the ligand, which can be considered as physisorbed. In Ag hydrosol

Table 1. Effective atomic charges, as calculated by natural bond order analysis. Pyridine (*Py*), pyrazolide (*Pz*$^-$)

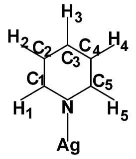

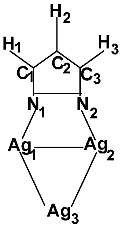

Atom	Pyridine	Py/Ag$^+$		Atom	Pyrazolide	Pz$^-$(Ag$_3$)$^+$
C_1	0.048	0.087		C_1	-.129	-.024
C_2	-.254	-.223		C_2	-.437	-.355
C_3	-.192	-.133		C_3	-.129	-.024
C_4	-.254	-.223		N_1	-.414	-.515
C_5	0.048	0.087		H_1	0.170	0.212
N	-.496	-.682		H_2	0.184	0.225
H_1	0.213	0.231		H_3	0.170	0.212
H_2	0.225	0.257		N_2	-.414	-.515
H_3	0.224	0.254		Ag_1		0.500
H_4	0.225	0.257		Ag_2		0.500
H_5	0.213	0.231		Ag_3		-.217
Ag		0.858				

an intense SPA band is observed in the UV–vis absorption spectrum at about 390 nm, relative to small spheroidal silver particles with average diameter of around 15 nm [22]. The colloidal aggregation, induced by addition of a ligand or by aging, affects the SPA, resulting in the appearance of a secondary band at longer wavelengths, due to larger silver particles. The presence of chloride anions adsorbed on silver usually prevents aggregation [23]. According to the electromagnetic enhancement effect [10], the excitation profiles of the SERS bands should follow the trend of the secondary plasmon resonance. Thus, by comparing the excitation profiles and the absorption spectra, it is possible to estimate the importance of the electromagnetic contribution for the SERS intensities. The SERS spectrum of Py, adsorbed on a silver colloid after addition of NaCl is shown in Fig. 2 and is compared with the normal Raman spectrum of pure liquid and with the calculated spectra of free Py and of the Py/Ag$^+$ complex. The SERS is dominated by two intense bands at about 1,008 and 1,036 cm^{-1}, corresponding to the ring-breathing and to the triangular-deformation modes, respectively. A remarkable point is that, as can be seen from Fig. 3, the SERS excitation profiles do not match the plasmon resonance bands of the salt-free colloid or of the hydrosol with chloride anions. This implies that the chemical effect due to the formation of Py/Ag charge-transfer complexes should have a strong effect on the SERS intensities in the present case, as is usually observed in Ag hydrosols activated by the coadsorption of halide anions [23]. The SERS spectrum closely resembles the Raman spectrum of the Ag(I)Py$_2$NO$_3$ coordination compound, concerning both the peak positions and the relative intensities (Table 2). The same was found to occur for other heteroaromatic ligands, like 2,2′-bipyridine [24], 2,2′-bipyrimidine [25] and 1,10-phenanthroline [26]. The calculated spectrum of the Py/Ag$^+$ complex (Fig. 2, spectrum d) closely reproduces the SERS spectral pattern and therefore can be considered as a simple but satisfactory model of chemisorbed Py. The frequencies and intensities calculated using density functional theory (DFT) are reported in Table 2 and are compared with experimental values. The assignment of free Py agrees with that proposed by Klots [27], except for the Raman band at 1,290 cm^{-1}, detected also in the IR spectrum at 1293 cm^{-1}, which is here assigned as a fundamental instead of the shoulder observed at 1,228 cm^{-1}, not detected in the IR spectrum. The band at about 1,580 cm^{-1} shown in Fig. 2, spectrum b, is due to the overlapping of the two normal modes calculated to be at 1,583 and 1,581 cm^{-1}, which correspond to the Raman bands observed in liquid Py at 1,573 and 1,582 cm^{-1}, respectively (Table 2). It is seen that, going from the isolated molecule to the surface complex, upshifts of the totally symmetric ring modes are obtained, in particular for the in-plane deformation (603 → 644 cm^{-1}), the breathing (969 → 1000 cm^{-1}), the triangular (1021 → 1038 cm^{-1}) and the ring C=C stretching (1581 → 1606 cm^{-1}) modes, in satisfactory agreement with the experimental findings. It is also seen that the intensities corresponding to the prominent bands at 1,008 and 1,036 cm^{-1}, calculated for the Py/Ag$^+$ complex, almost equalise, as observed in the SERS spectrum. An intensity decrease of the ring deformation mode at around 650 cm^{-1} in the Py/Ag$^+$ complex is also in fair agreement with the SERS experiment.

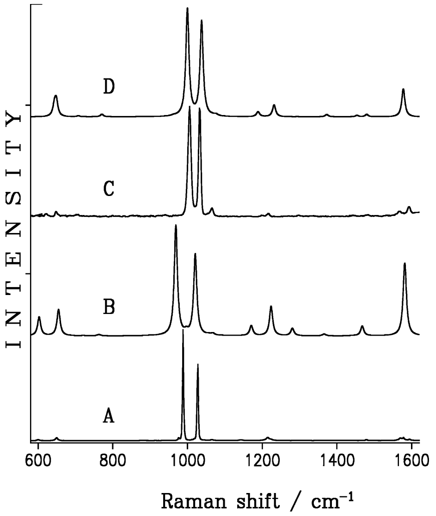

Fig. 2. **A** Raman spectrum of liquid pyridine (exciting line 514.5 nm); **B** calculated Raman spectrum of pyridine; **C** Raman spectrum of pyridine adsorbed on a Ag colloid (exciting line 514.5 nm); **D** calculated Raman spectrum of a pyridine/Ag$^+$ complex. The calculated bands are shown as Lorentzian shapes having 10-cm^{-1} bandwidth

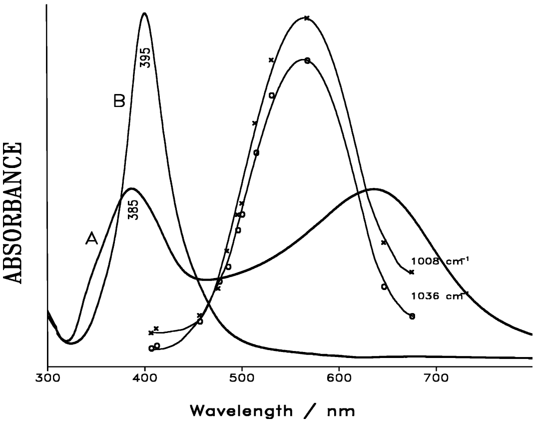

Fig. 3. UV–vis extinction spectra of Ag colloids in the presence of 10^{-3} M pyridine: **A** salt-free Ag colloid; **B** Ag colloid with 10^{-3}M NaCl. The surface-enhanced Raman scattering (*SERS*) excitation profiles of pyridine are also shown for the two strong bands at 1,008 and 1,036 cm^{-1}

Pyrazolide

The SERS spectrum of Pz$^-$ adsorbed on a silver colloid is shown in Fig. 4 and is compared with the Raman spectrum of the Ag(I) coordination compound. This

Table 2. Calculated (scaling factor 0.9833) and observed frequencies of Py, of Py adsorbed on silver and of the Py/Ag$^+$ complex. Calculated relative Raman intensities reported in *parentheses*

Py, liquid			Py	Py	Py/Ag$^+$	PyAg(I) complex, solid	Py on Ag colloid
Species	Assignment[a]	Obs. Raman[b]	Calc.	Obs. Raman[b]	Calc.	Obs. Raman[b]	Obs. SERS[b]
					201 (5.6)		210 br[c]
A_2	ν (13)	379[a]	381 (0.1)		392 (0.2)		
B_1	ν (27)	407 w	419 (1.9)		427 (0.6)		
A_1	ν (10)	604 w/m	603 (17.0)	615 w/m	644 (10.2)	623 vw	623 w
B_2	ν (22)	653 m	655 (23.8)	649 m	649 (14.2)	650 w	649 w/m
B_1	ν (26)	709 vvw	721 (0.3)		708 (0.9)	709 w	708 w
B_1	ν (25)	750 vvw	763 (1.2)		771 (2.4)		
A_2	ν (12)	885 w	901 (0.1)		892 (0.1)	876vw	
B_1	ν (24)	942 vw	947 (0.1)		963 (0.6)	942vw	942 vw
A_1	ν (9)	992 vvs	969 (100.0)	1,000 vvs	1,000 (100.0)	1,006 vvs	1,008 vvs
A_2	ν (11)	980 sh	997 (2.6)		1,004 (0.1)		
A_1	ν (8)	1,031 vs	1,021 (73.7)	1,032 vs	1,038 (88.4)	1,034 vvs	1,036 vvs
B_1	ν (23)	1,020 vvw	1,027 (0.1)		1,044 (0.0)		
B_2	ν (21)	1,052 vvw	1,056 (0.9)		1,077 (1.4)		
A_1	ν (7)	1,069 w	1,068 (1.8)	1,064 w	1,067 (0.5)	1,067 m	1,069 m
B_2	ν (20)	1,150 w	1,171 (9.1)		1,189 (4.7)	1,198 sh	1,197 sh
A_1	ν (6)	1,218 m	1,224 (26.8)	1,216 m	1,232 (11.1)	1,217 m	1,220 m
B_2	ν (19)	1,290[a]	1,281 (6.7)		1,295 (0.1)	1,297 vs	1,299 vw
B_2	ν (18)	1,356 vvw	1,366 (1.6)		1,373 (2.2)		
B_2	ν (17)	1,438 vvw	1,440 (0.2)		1,454 (1.4)	1,454 w	1,452 vw
A_1	ν (5)	1,483 w	1,468 (8.8)	1,480 vw	1,480 (2.2)	1,486 m	1,487 w
B_2	ν (16)	1,573 w/m	1,583 (31.4)	1,574 w/m	1,578 (26.2)	1,575 w/m	1,575 w/m
A_1	ν (4)	1,582 m	1,581 (37.2)	1,592 m	1,606 (34.7)	1,595 m	1,599 m

[a] Ref. [27]
[b] 514.5-nm exciting line
[c] Salt-free Ag colloid

latter consists of Pz$^-$ anions bound to two Ag$^+$ ions to form polymeric chains. It can be seen that the SERS spectrum of Pz$^-$, in contrast with findings in Py, is distinctly different, as far as the relative intensities are concerned, from the spectrum of the Ag(I) complex. In particular, the 1,484-cm^{-1} band appears as the strongest mode in the SERS spectrum, while its intensity is very low in the complex. A DFT calculation of the Raman spectrum of the Ag(I) complex, modelled as a Pz$^-$(Ag$^+$)$_2$ adduct, was performed and the results are reported in Table 3 and are also shown in Fig. 4. It can be seen that the agreement with the experimental values is quite satisfactory, in particular as far as the pattern of the more prominent bands is concerned.

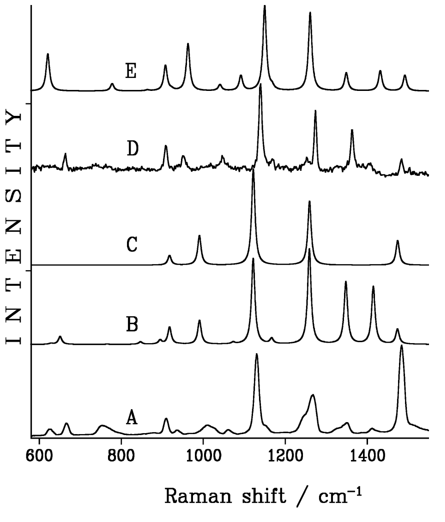

Fig. 4. A Raman spectrum of pyrazolide adsorbed on a Ag colloid (exciting line 514.5 nm); **B** calculated Raman spectrum of a pyrazolide/(Ag$_3$)$^+$ complex; **C** as **B**, by considering only the contribution of the dynamic polarisability normal to the metal surface; **D** Raman spectrum of the solid Ag(I)–pyrazolide complex (exciting line 514.5 nm); **E** calculated Raman spectrum of the pyrazolide/(Ag$^+$)$_2$ complex. The calculated bands are shown as Lorentzian shapes having 10-cm^{-1} bandwidth

In previous work [9] a DFT calculation of the frequencies for a model of the Pz$^-$/Ag adduct, consisting of the anion bound to two adsorption sites of the metal surface with a single positive charge, Pz$^-$(Ag$_2$)$^+$, was reported. This calculation was extended in the present work to obtain the relative SERS intensities as well (Table 3). The adduct was modelled as the anion bound to a cluster of three silver atoms, Pz$^-$(Ag$_3$)$^+$. This allows the computation of the Raman intensities in a closed-shell system. The calculated intensities, obtained as the total Raman intensities averaged over all spatial orientations, as indicated in the previous section, are compared in Fig. 4 with those observed in the SERS experiment. It can be seen that the fit is rather poor and in particular the intensities of the bands at 1,263, 1,350 and 1,409 cm^{-1} are largely overestimated in the calculations, while the most intense SERS band at 1,484 cm^{-1} is predicted as only a weak band. However, it should be noted that Pz$^-$ adsorbed on silver has C_{2v} symmetry with the z symmetry axis perpendicular to the surface.

Table 3. Calculated (scaling factor 0.9833) and observed frequencies of Pz^- adsorbed on silver and of the Pz^-/Ag(I) complex. Calculated relative Raman intensities reported in *parentheses*

$Pz^-(Ag_3)^+$		$Pz^-(Ag_2)^+$	Pz^- on Ag colloid	$Pz^-(Ag^+)_2$	Pz^-Ag(I) complex, solid
Species	Calc.	Calc.	Obs. SERS[a]	Calc.	Obs. Raman[a]
A_1	238 (9.4)	234	235 br	264 (21.4)	248 w/m
B_2	629 (1.2)	628	625 w	621 (5.6)	
A_2	651 (9.2)	647	665 m	621 (38.0)	664 w/m
B_2	766 (0.3)	762	758 w,br	778 (8.7)	768 w
A_2	847 (2.8)	846		864 (1.1)	
B_2	895 (4.6)	895		923 (1.4)	
A_1	918 (19.9)	917	908 m	908 (29.8)	908 m
B_1	943 (0.4)	942		963 (55.4)	951 m
A_1	991 (27.8)	999	1,009 w,br	1,041 (7.1)	1,046 w/m
B_1	1,073 (1.9)	1,072	1,064 w	1,092 (17.7)	1,102 w
A_1	1,122 (100.0)	1,125	1,129 vs	1,150 (100.0)	1,140 vs
B_1	1,167 (6.1)	1,161	1,160 sh	1,168 (3.9)	1,168 w/m
A_1	1,259 (111.1)	1,261	1,263 s	1,261 (91.9)	1,274 s
B_1	1,348 (72.7)	1,344	1,350 w/m	1,349 (21.0)	1,364 m
B_1	1,415 (67.0)	1,413	1,409 w	1,432 (23.7)	1,408 m
A_1	1,474 (17.4)	1,473	1,484 vs	1,492 (18.5)	1,484 m

[a]514.5-nm exciting line

According to the electromagnetic theory [4] the intensity enhancement of the vibrational modes should be associated with the magnitude of the *zz* component of the dynamic polarizability. The *zz*-component contribution to the calculated Raman intensities is shown in Fig. 4 and it can be seen that, even if a fit with experimental data is not obtained, at least the changes of the spectral features are in the expected direction. It is possible that an improvement of the ligand–surface interaction is necessary to reproduce the relative SERS intensities. The present results give an indication that in the Pz^- case the electromagnetic effect could be predominant. To find evidence for this hypothesis, the SERS excitation profiles of Pz^- in salt-free Ag hydrosol were measured. The results are shown in Fig. 5 and are compared with the UV–vis absorption spectrum, while in Fig. 6 the SERS spectra of Pz^- with different exciting lines are shown. It can be seen that the SERS excitation profiles closely follow the shape of the secondary plasmon resonance. This confirms that in the present case there is a predominance of the electromagnetic enhancement mechanism. The enhancement is particularly evident for the 1,484-cm^{-1} band, whose intensity overcomes that of the 1,129-cm^{-1} band by excitation with redshifted laser lines. In contrast, the intensity of the 1,263-cm^{-1} band continuously decreases as the wavelength of the exciting line increases. Moreover, the agreement between experimental and calculated relative intensities tends to improve as the exciting wavelength is shifted to the blue (Fig. 6). In fact the 1,484-cm^{-1} band decreases in intensity, whereas the 1,263-cm^{-1} band becomes the strongest SERS band. Actually, when the exciting line is far from resonance with the secondary plasmon resonance of the metal particles, the predominance of the electromagnetic enhancement effect weakens and the chemical contribution becomes nonnegligible.

Finally, in the low-frequency region the ligand–Ag stretching modes usually occur. As shown in Fig. 7, the

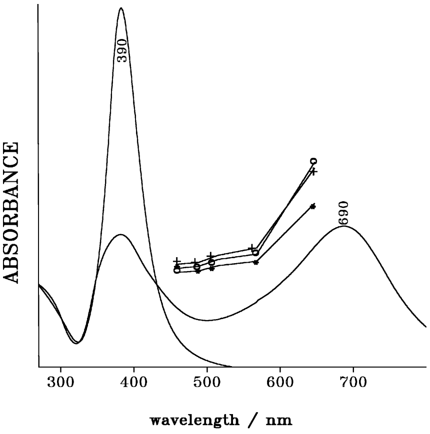

Fig. 5. UV–vis extinction spectra of salt-free Ag colloids, in the absence of ligand and in the presence of 10^{-3} M pyrazole. The SERS excitation profiles of pyrazolide, obtained with different laser exciting lines (457.9, 488.0, 514.5, 568.2, 647.1 nm), are also shown: (*) 1,129-cm^{-1} band (*stars*), 1484-cm^{-1} band (*circles*); 908-cm^{-1} band (*crosses*) (intensities multiplied by 10)

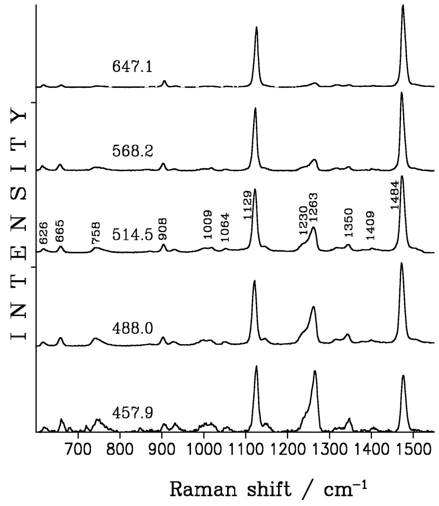

Fig. 6. SERS spectra of pyrazolide adsorbed on a Ag colloid, with different laser exciting lines

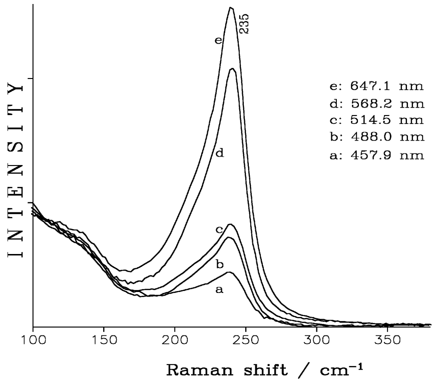

Fig. 7. SERS spectra of pyrazolide adsorbed on Ag colloid, in the low-frequency region

Ag–Pz^- stretching mode is observed as a broad band centred at around 235 cm^{-1}. This vibration exhibits a weak intensity in the DFT calculation of the $Pz^-(Ag_3)^+$ complex and should be described as a rigid translation of the molecule relative to the silver substrate, very much like the motion of a physisorbed molecule. Experimentally, the intensity of this mode strongly increases when the exciting line is redshifted. Therefore, this mode mainly experiences the electromagnetic enhancement effect, as previously observed for 2,2′-bipyrimidine in a Ag hydrosol [25].

Conclusions

In the present paper the SERS spectra of Py and of Pz^- adsorbed on silver colloids were discussed with the help of DFT calculations for the Raman frequencies and intensities of surface complexes consisting of ligands bound to small Ag clusters or even to a single Ag atom. Even though the present discussion was confined to consider relative intensities, useful information was obtained. In the case of Py, the calculated Raman intensities of the model adduct compare satisfactorily with the relative intensities of the SERS spectrum. This is correlated with the importance of the chemical effect, as demonstrated by considering the SERS excitation profiles. In contrast, these latter profiles show that the electromagnetic mechanism predominates in the SERS enhancement of Pz^-. In concomitance with this, the relative intensities of the SERS spectrum differ significantly from those calculated for the adduct of Pz^- with Ag clusters, independent of the cluster size.

Acknowledgements The authors gratefully thank the Italian Ministero dell'Istruzione, Universita' e Ricerca and the Consiglio Nazionale delle Ricerche for financial support to the "Progetto Finalizzato Materiali Speciali II".

References

1. Chang RK, Furtak TE (eds) (1981) Surface-enhanced Raman scattering. Plenum, New York
2. Otto A (1984) In: Cardona M, Güntherodt G (eds) Light scattering in solids, vol. IV. Springer, Berlin Heidelberg New York, chap 6
3. Campion A, Kambhampati P (1998) Chem Soc Rev 27:241
4. (a) Moskovits M (1982) J Chem Phys 77:4408; (b) Moskovits M, Suh JS (1984) J Phys Chem 88:5526
5. Mrozek I, Otto A (1990) J Electron Spectrosc Relat Phenom 54:895
6. Campion A, Ivanecky JE III, Child CM, Forster M (1995) J Am Chem Soc 117:11807
7. Aroca RF, Clavijo RE, Halls MD, Schlegel HB (2000) J Phys Chem A 104:9500
8. Bigotto A, Pergolese B (2001) J Raman Spectrosc 32:953
9. Cardini G, Muniz-Miranda M (2002) J Phys Chem B 106:6875
10. Creighton JA, Blatchford CG, Albrecht MG (1979) J Chem Soc Faraday Trans II 75:790
11. Muniz-Miranda M, Neto N, Sbrana G (1986) J Mol Struct 143:275
12. Cooney RP, Howard MW, Mahoney MR (1981) Chem Phys Lett 79:459
13. Buchner E (1889) Chem Ber 22:842
14. Frisch MJ, Trucks GW, Schlegel HB, Scuseria GE, Robb MA, Cheeseman JR, Zakrzewski VG, Montgomery JA Jr, Stratmann RE, Burant JC, Dapprich S, Millam JM, Daniels AD, Kudin KN, Strain MC, Farkas O, Tomasi J, Barone V, Cossi M, Cammi R, Mennucci B, Pomelli C, Adamo C, Clifford S, Ochterski J, Petersson GA, Ayala PY, Cui Q, Morokuma K, Malick DK, Rabuck AD, Raghavachari K, Foresman JB, Cioslowski J, Ortiz JV, Stefanov BB, Liu G, Liashenko A, Piskorz P, Komaromi I, Gomperts R, Martin RL, Fox DJ, Keith T, Al-Laham MA, Peng CY, Nanayakkara A, Gonzalez C, Challacombe M, Gill PMW, Johnson BG, Chen W, Wong MW, Andres JL, Head-Gordon M, Replogle ES, Pople JA (1998) Gaussian 98. Gaussian, Pittsburgh, PA
15. Becke AD (1988) Phys Rev A 33:3098
16. Lee C, Yang W, Parr RG (1988) Phys Rev B 37:785
17. Dunning TH Jr, Hay PJ (1976) In: Schaefer HF III (ed) Modern theoretical chemistry, vol 3. Plenum, New York, pp
18. (a) Hay PJ, Wadt WR (1985) J Chem Phys 82:270; (b) Wadt WR, Hay PJ (1985) J Chem Phys 82:284; (c) Hay PJ, Wadt WR (1985) J Chem Phys 82:299
19. Wilson EB, Decius JC, Cross PC (eds) (1955) Molecular vibrations. McGraw-Hill, London
20. Kerker M, Wang D-S, Chew H (1980) Appl Opt 19:4159
21. Wang D-S, Kerker M (1981) Phys Rev B 24:1777
22. Nabiev IR, Savchenko VA, Efremov ES (1983) J Raman Spectrosc 13:375
23. Muniz-Miranda M, Sbrana G (1996) J Raman Spectrosc 27:105
24. Kim M, Itoh K (1987) J Phys Chem 91:126
25. Sbrana G, Neto N, Muniz-Miranda M, Nocentini M (1990) J Phys Chem 94:3706
26. Muniz-Miranda M (2000) J Phys Chem A 104:7803
27. Klots TD (1998) Spectrochim Acta Part A 54:1481